

## STAR FORMATION EFFICIENCY AT HIGH Z AND SUBGALACTIC SCALES

J. Freundlich<sup>1</sup>, F. Combes<sup>1</sup>, L. J. Tacconi<sup>2</sup>, M. C. Cooper<sup>3</sup>, R. Genzel<sup>2,4,5</sup>, R. Neri<sup>6</sup> and the PHIBSS consortium

**Abstract.** Massive galaxies in the distant Universe form stars at much higher rates than their local counterparts. Although direct resolution of the star forming regions of these galaxies is still a challenge, recent molecular gas observations at the IRAM Plateau de Bure interferometer enable us to study the star formation efficiency at sub-galactic scales around  $z = 1.2$ . We present a method to obtain the gas and star formation rate (SFR) surface densities of ensembles of clumps within galaxies at this redshift, and derive a spatially resolved Kennicutt-Schmidt (KS) relation at a scale of about 8.5 kpc. This method is based on the identification of these structures in position-velocity diagrams corresponding to slices within the galaxies, even though the corresponding scales are not resolved. The data globally indicates an average depletion time of 1.9 Gyr, but with significant variations from point to point within the galaxies.

Keywords: galaxies: evolution, galaxies: high redshift, galaxies: ISM, galaxies: starburst

### 1 Introduction

Our Milky Way only forms a few stars per year, similar to most nearby spiral galaxies. But ten billion years ago, between redshifts 1 and 3, observed galaxies formed their stars at rates up to ten times higher (Noeske et al. 2007, Daddi et al. 2007). Stars are formed from cold gas clouds which collapse due to their self gravity. A high star formation rate (SFR) thus means a significant gas supply, either brought by major mergers or by continuous processes, for example through filaments of the cosmic web (Kereš et al. 2005, Dekel et al. 2009). Observations show that high redshift galaxies are indeed more gas-rich than their low redshift counterparts, their gas fraction being as high as 30-40% (Tacconi et al. 2010, 2013). This could explain on its own the high SFR, but the star formation processes could also be more efficient, and we would like to characterize them at their relevant sub-galactic scales. High redshift galaxies do not resemble our Galaxy or the galaxies in our neighborhood, as their disk is fragmented to a number of giant molecular clouds, or clumps, where most of the star formation occurs. These structures have sizes of about 1 kpc, masses up to  $10^9 M_{\odot}$ , and contribute 10-25% of the galaxy luminosity (Förster Schreiber et al. 2011). Are the star formation processes qualitatively different in high redshifts clumps than in their low redshift counterparts ?

As stars are formed from cold molecular gas, the SFR density should significantly depend on the gas density. The relationship between the two quantities describes the star formation efficiency, and has often been written as a simple power law (Schmidt 1959, Kennicutt 1998a). We would like to obtain a corresponding Kennicutt-Schmidt (KS) relation for clumps or ensembles of clumps of high redshift galaxies, and compare it to similar observations at low redshift (e.g. Bigiel et al. 2011). Genzel et al. (2010) and Tacconi et al. (2010) study the global properties of galaxies at  $z=1.2$ , and we select four galaxies out of their PHIBSS sample (Tacconi et al. 2010). These galaxies are not experiencing major mergers and are typical  $z=1.2$  massive star-forming galaxies,

---

<sup>1</sup> LERMA, Observatoire de Paris, CNRS, 61 av. de l'Observatoire, 75014 Paris, France

<sup>2</sup> Max-Planck-Institute für extraterrestrische Physik (MPE), Giessenbachstrasse 1, 85748 Garching, Germany

<sup>3</sup> Dept. of Physics & Astronomy, Frederick Reines Hall, University of California, Irvine, CA 92697, USA

<sup>4</sup> Dept. of Physics, Le Conte Hall, University of California, CA 94720 Berkeley, USA

<sup>5</sup> Dept. of Astronomy, Campbell Hall, University of California, CA 94720 Berkeley, USA

<sup>6</sup> IRAM, 300 rue de la Piscine, 38406 St. Martin d'Herès, Grenoble, France

with stellar masses above  $3 \times 10^{10} M_{\odot}$ . High resolution CO observations with the IRAM Plateau de Bure interferometer and Keck DEEP2 spectra enable us to fathom star formation processes at scales lower than the galaxy size. We first determine the total mass of gas and the global SFR of the selected galaxies, then isolate sub-structures through position-velocity diagrams, and finally plot a KS diagram at their sub-galactic scale. More details can be found in Freundlich et al. (2013).

## 2 Determining global properties of galaxies at $z=1.2$

### 2.1 Determination of the total mass of gas

The IRAM Plateau de Bure interferometer is able to observe the CO molecular gas of high redshift galaxies, from which we can determine their total mass of gas. We assume that the CO(3-2) rotational line luminosity is directly proportional to the total mass of gas, and we use a Milky Way like conversion factor  $\alpha = 8.7$  between the two (Tacconi et al. 2010):

$$\left(\frac{M_{\text{gas}}}{M_{\odot}}\right) = \alpha \left(\frac{L_{\text{CO}(3-2)}}{\text{K km s}^{-1} \text{pc}^2}\right)$$

More precisely, we use a conversion factor of 3.2 between the  $\text{H}_2$  mass and the CO(1-0) luminosity, assume a factor 2 for the CO(3-2)/CO(1-0) luminosity ratio, and further correct by a factor 1.36 to account for interstellar helium. The spatial resolution attained by the IRAM Plateau de Bure interferometer is around  $1''$ ; about 8.5 kpc at  $z=1.2$ .

### 2.2 Determination of the global SFR

The  $\text{H}\alpha$  recombination line is the most direct and reliable tracer of young massive stars, and thus of the SFR (Kennicutt 1998b). But for  $z=1.2$  galaxies, this line lies in the middle of a low atmospheric transmission band, so ground based spectroscopy is impossible for our set of galaxies, and we have to use different methods to determine the SFR.

We notably estimate the SFR from the collisionally excited [OII] line, using DEEP2 spectra. Even though the [OII] line luminosity is not directly coupled to the ionizing luminosity, it is possible to establish it empirically as a quantitative SFR tracer (Kennicutt 1998b, Kewley et al. 2004):

$$\left(\frac{\text{SFR}}{M_{\odot} \text{ yr}^{-1}}\right) \simeq 3.5 \cdot 10^{-8} \left(\frac{L_{[\text{OII}]}}{L_{\odot}}\right)$$

The Keck DEEP2 spectra are calibrated with CFHT photometric data and have a spatial resolution comprised between  $0.6$  and  $1.0''$ . Dust extinction is determined from spectral energy distributions (SED) obtained by `kcorrect` from CFHT photometric data (Blanton & Roweiss 2007).

Other methods to determine the SFR include an empirical [OII] calibration in terms of B-band luminosity (Moustakas et al. 2006) and a combined UV and IR calibration (Wuyts et al. 2011, Tacconi et al. 2013). The former method is assumed to remove on average the systematic effects of reddening and metallicity and to reduce the scatter in the resulting SFR values, whereas the latter method is expected to be the most reliable in the absence of  $\text{H}\alpha$  measurements. Indeed, UV light directly traces unobscured star formation and IR  $24 \mu\text{m}$  emission originates in small dust grains heated by the UV photons, the combination of the two thus tracing unobscured and obscured star formation at the same time. The SFR values obtained with the three methods differ up to  $3\sigma$ , which shows how the SFR calibration is an important source of uncertainties.

## 3 Star formation at sub-galactic scales

The kpc-sized clumps of high redshift galaxies are smoothed out at DEEP2 and IRAM resolutions, but spectroscopy helps separate different components, thanks to their kinematics. DEEP2 spectra indeed correspond to position-velocity diagrams (PV diagrams) along the galaxy major axis (Davis et al. 2007), and we are able to separate smoothed ensembles of clumps along the velocity axis. The size of these substructures corresponds to the angular resolution available in both CO and [OII] spectroscopy; i.e.,  $1-1.5''$ , or about 8.5 kpc at  $z=1.2$ . Figure 1 compares the [OII] PV diagram with the corresponding slice in IRAM CO(3-2) data for one of the four galaxies (named EGS13004291 in the AEGIS terminology). The white horizontal lines show the boundaries

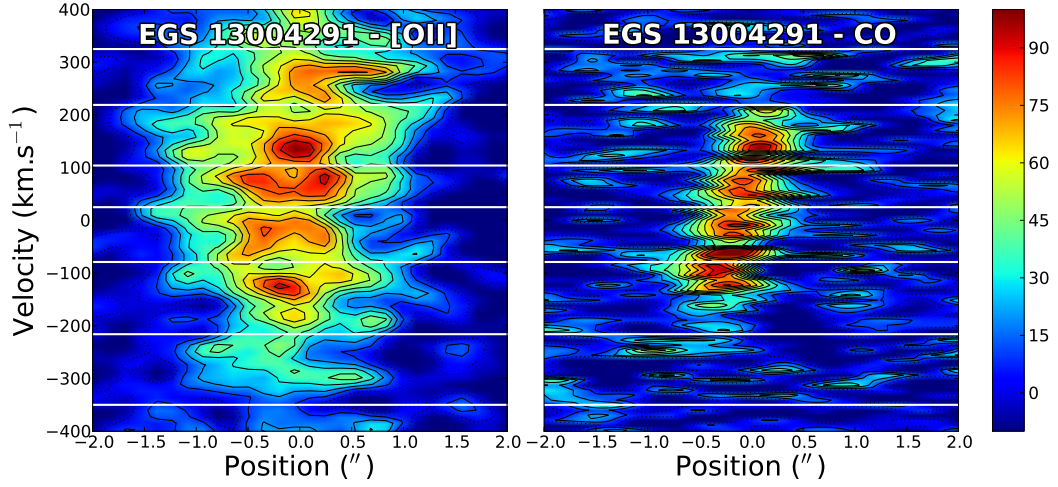


**Fig. 1.** [OII] and CO line luminosities of one galaxy of our sample (EGS13004291) in position-velocity planes corresponding to the DEEP2 slit. Smoothed ensembles of clumps are separated by eye along the vertical axis, as shown with the white horizontal lines. One arc second corresponds approximately to 8.5 kpc.

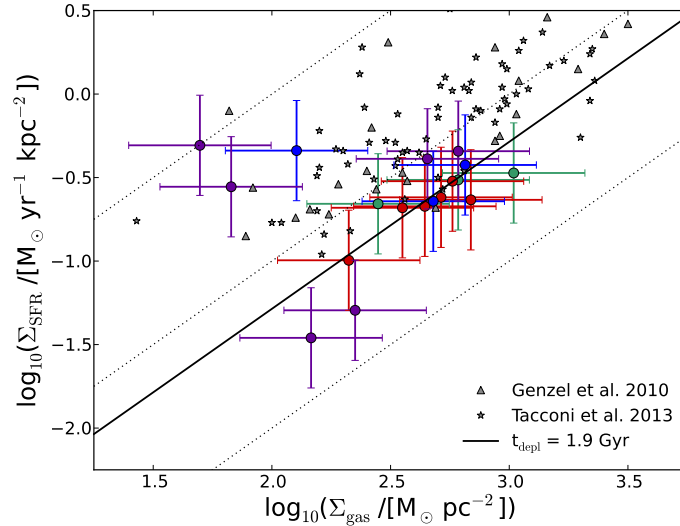


**Fig. 2.** Kennicutt-Schmidt diagram for 1'' ensembles of clumps of four galaxies at  $z=1.2$ , using the Kewley et al. (2004) [OII] SFR calibration. The dotted diagonal lines correspond to constant gas depletion times of 0.1, 1, and 10 Gyr from top to bottom, and the solid black line to a constant depletion time equal to the mean depletion time of the ensembles of clumps,  $t_{\text{depl}} = 1.9$  Gyr. The gray data points from Genzel et al. (2010) and Tacconi et al. (2013) are indicated for comparison with whole galaxies.

between the different substructures, determined by eye. We assume that the mass of gas and the SFR of each ensemble of clumps are respectively proportional to the integrated luminosity in the CO and [OII] PV diagrams, so we can deduce the mass and SFR surface densities averaged over areas of about 1'' in diameter.

The mean depletion time ( $t_{\text{depl}} = M_{\text{gas}}/\text{SFR}$ ) for these ensembles of clumps is equal to  $1.9 \pm 0.3$  Gyr, which is comparable to low redshift observational results (Kennicutt 1998b, Genzel et al. 2010, Saintonge et al. 2011, Tacconi et al. 2013, Bigiel et al. 2008, 2011). Figure 2 displays the corresponding resolved KS diagram. The data points scatter around the line of constant depletion time equal to 1.9 Gyr, but there are significant variations from point to point within the galaxies. This suggests that the star formation scaling laws could be different from one ensemble of clumps to the next within a galaxy, even if the scatter is comparable to the  $\sim 0.3$  dex observed for resolved local galaxies (Bigiel et al. 2008, 2011).

The main uncertainties come from the SFR calibration, the determination of the extinction and from the conversion factors used to convert the CO luminosity in a mass of gas. These latter quantities are also expected to vary within a single galaxy, and thus influence the slope of the KS relation (Koda et al. 2012, Genzel et al. 2013). Although the three methods to determine the SFR give very different values, it does not affect much the final shape of the KS relation.

#### 4 Conclusion

We have shown that various ensembles of clumps could be separated by their kinematics in PV diagrams, even though the corresponding scales were not resolved. We are able to draw a KS relation for these ensembles of clumps in four galaxies, and our sample is compatible with a constant depletion time of 1.9 Gyr. This adds to the growing evidence that the star formation scaling laws, and thus the star formation processes, are not significantly different at high redshift than in the local Universe. Nevertheless, this method should be applied to a more significant sample of high redshift galaxies to obtain more statistically robust results, notably within the upcoming IRAM PHIBSS2 Legacy Program.

#### References

- Bigiel, F., Leroy, A., Walter, F., et al. 2008, *ApJ*, 136, 2846  
Bigiel, F., Leroy, A., Walter, F., et al. 2011, *ApJ*, 730, L13  
Blanton, M. R., & Roweis, S. 2007, *ApJ*, 133, 734  
Daddi, E., Dickinson, M., Morrison, G., et al. 2007, *ApJ*, 670, 156  
Davis, M., Guhathakurta, P., Konidakis, N. P., et al. 2007, *ApJ*, 660, L1  
Dekel, A., Birnboim, Y., Engel, G., et al. 2009, *Nature*, 457, 451D  
Förster Schreiber, N. M., Shapley, A. E., Genzel, R., et al. 2011, *ApJ*, 739, 45F  
Freundlich, J., Combes, F., Tacconi, L. J., et al. 2013, *A&A*, 553, A130  
Genzel, R., Tacconi, L. J., Gracia-Carpio, J., et al. 2010, *MNRAS*, 407, 2091  
Genzel, R., Tacconi, L. J., Kurk, J., et al. 2013, *ApJ*, 773, 68G  
Kennicutt, R. C. Jr. 1998a, *ApJ*, 498, 541  
Kennicutt, R. C. Jr., 1998b *ARA&A*, 36, 189  
Kereš, D., Katz, N., Weinberg, D. H., & Davé, R. 2005, *MNRAS*, 363, 2K  
Kewley, L. J., Geller, M. J., & Jansen, R. A. 2004, *ApJ*, 127, 2002  
Koda, J., Scoville, N., Hasegawa, T., et al. 2012, *ApJ*, 761, 41K  
Moustakas, J., Kennicutt, R. C., & Tremonti, C. 2006, *ApJ*, 642, 775M  
Noeske, K. G., Weiner, B. J., Faber, S., et al. 2007, *ApJ*, 660, L43  
Saintonge, A., Kauffmann, G., Wang, J., et al. 2011, *MNRAS*, 415, 61S  
Schmidt, M. 1959, *ApJ*, 129, 243S  
Tacconi, L. J., Genzel, R., Neri, R., et al. 2010, *Nature*, 463, 781T  
Tacconi, L. J., Neri, R., Genzel, R., et al. 2013, *ApJ*, 768, 74T  
Wuyts, S., Förster Schreiber, N. M., van der Wel, A., et al. 2011, *ApJ*, 742, 96W